

# Nuclear Factor I Gene Expression in the Developing Forebrain

CÉLINE PLACHEZ,<sup>1</sup> CHARLOTTA LINDWALL,<sup>2</sup> NANA SUNN,<sup>2</sup> MICHAEL PIPER,<sup>2</sup>  
 RANDAL X. MOLDRICH,<sup>2</sup> CHRISTINE E. CAMPBELL,<sup>3</sup> JASON M. OSINSKI,<sup>3</sup>  
 RICHARD M. GRONOSTAJSKI,<sup>3</sup> AND LINDA J. RICHARDS<sup>1,2\*</sup>

<sup>1</sup>University of Maryland, Baltimore, School of Medicine, Baltimore, Maryland, USA  
<sup>2</sup>University of Queensland School of Biomedical Sciences and Queensland Brain Institute,  
 St Lucia, Queensland, Australia  
<sup>3</sup>Department of Biochemistry and the Program in Neuroscience, State University of  
 New York at Buffalo, New York, USA

## ABSTRACT

Three members of the Nuclear Factor I (*Nfi*) gene family of transcription factors; *Nfia*, *Nfib*, and *Nfix* are highly expressed in the developing mouse brain. *Nfia* and *Nfib* knockout mice display profound defects in the development of midline glial populations and the development of forebrain commissures (das Neves et al. [1999] Proc Natl Acad Sci U S A 96:11946–11951; Shu et al. [2003] J Neurosci 23:203–212; Steele-Perkins et al. [2005] Mol Cell Biol 25:685–698). These findings suggest that *Nfi* genes may regulate the substrate over which the commissural axons grow to reach targets in the contralateral hemisphere. However, these genes are also expressed in the cerebral cortex and, thus, it is important to assess whether this expression correlates with a cell-autonomous role in cortical development. Here we detail the protein expression of NFIA and NFIB during embryonic and postnatal mouse forebrain development. We find that both NFIA and NFIB are expressed in the deep cortical layers and subplate prenatally and display dynamic expression patterns postnatally. Both genes are also highly expressed in the developing hippocampus and in the diencephalon. We also find that principally neither NFIA nor NFIB are expressed in callosally projecting neurons postnatally, emphasizing the role for midline glial cell populations in commissure formation. However, a large proportion of laterally projecting neurons express both NFIA and NFIB, indicating a possible cell-autonomous role for these transcription factors in corticospinal neuron development. Collectively, these data suggest that, in addition to regulating the formation of axon guidance substrates, these genes also have cell-autonomous roles in cortical development. J. Comp. Neurol. 508:385–401, 2008. © 2008 Wiley-Liss, Inc.

**Indexing terms:** cortical development; hippocampus; midline glia; transcription factor; cortical layers; telencephalon; NFI

The nuclear factor I (NFI) gene family has four members in vertebrates: *Nfia*, *Nfib*, *Nfic*, and *Nfix*, sharing a conserved sequence of 220 amino acids in the N-terminal domain. Different isoforms are generated by multiple alternative splicing of individual NFI genes (Santoro et al., 1988; Inoue et al., 1990; Apt et al., 1994). The *Nfi* genes encode transcription factors in birds and mammals (Gil et al., 1988; Meisterernst et al., 1988; Paonessa et al., 1988; Santoro et al., 1988; Inoue et al., 1990; Rupp et al., 1990). They are specific DNA-binding proteins that were identified through their roles in adenoviral DNA replication, both in vitro (Nagata et al., 1982; Hurwitz et al., 1985; Leegwater et al., 1985; Rosenfeld et al., 1987) and in vivo (Hay, 1985; Wang and Pearson, 1985). The roles of the

NFI gene family in transcription and development have been reviewed (Gronostajski, 2000).

Grant sponsor: National Health and Medical Research Council (NHMRC); Grant number: 401616.

C.P. and C.L. contributed equally to this article.

\*Correspondence to: Assoc. Prof. Linda J. Richards, Queensland Brain Institute, University of Queensland, St Lucia, Queensland, 4072, Australia. E-mail: richards@uq.edu.au

Received 5 April 2007; Revised 22 June 2007; Accepted 19 December 2007

DOI 10.1002/cne.21645

Published online in Wiley InterScience (www.interscience.wiley.com).

Two members of the NFI gene family, *Nfia* and *Nfib*, are involved in brain wiring during development (das Neves et al., 1999; Shu et al., 2003; Steele-Perkins et al., 2005). Direct evidence of a role for NFI proteins in brain development comes from phenotypic analyses of *Nfia* (das Neves et al., 1999; Shu et al., 2003) and *Nfib* (Steele-Perkins et al., 2005) knockout mice. Disruption of either gene on a C57Bl/6 background causes perinatal lethality. In the case of *Nfib* mutants, lethality is due to defects in lung maturation (Steele-Perkins et al., 2005), whereas the cause for perinatal lethality in *Nfia* mutants is unknown. Also, both *Nfia* and *Nfib* knockouts display a significant loss of telencephalic midline glial populations (the glial wedge, GW; indusium griseum glia, IGG; and the subcallosal, or glial, sling, SS). Concomitant with the disruption in formation of these midline populations are malformations in the major forebrain commissures, particularly the corpus callosum and the hippocampal commissure (Shu et al., 2003; Steele-Perkins et al., 2005).

Recently, *Nfia* and *Nfib* have been shown to be potential downstream candidates of the transcription factors *Emx2*, *Pax6*, and *Neurogenin2* (Mattar et al., 2004; Gangemi et al., 2006; Holm et al., 2007). In each case, differential screens between wildtype and knockout tissue revealed that the *Nfi* genes were downregulated in the knockout tissue of either *Emx2*, *Pax6*, or *Neurogenin2*, indicating their likely role as downstream targets of these genes. *Emx2*, *Pax6*, and *Neurogenin2* are essential for forebrain patterning, neuronal and glial differentiation, and stem cell formation (Bishop et al., 2000; Muzio et al., 2002a,b; Muzio and Mallamaci, 2003; Hand et al., 2005; Britz et al., 2006), but how NFI proteins contribute to these cellular processes has not yet been clarified. An expression analysis of the mRNA of each *Nfi* gene has previously revealed that they exhibit unique but overlapping patterns of expression during mouse development. High mRNA levels were observed in brain, heart, lung, muscle, liver, and kidney (Chaudhry et al., 1997). However, any functional studies of the *Nfi* genes also require a detailed analysis of NFI protein expression. Here, using antibodies specific for either NFIA or NFIB, we examine the protein expression of these proteins during development of the mouse telencephalon. Additionally, using double labeling, we demonstrate that NFIA and NFIB are expressed in specific cell populations. Both proteins are expressed in laterally but not medially projecting cortical neurons. Prenatally, little or no NFIA or NFIB expression was found in interneurons, but importantly at this stage, low levels of both proteins were observed in the ventricular zone (VZ), indicating a role for these proteins in progenitor cells. The specific, overlapping, and distinct patterns of NFIA and NFIB expression in different forebrain regions at different developmental stages indicates possible functional roles in the development of specific forebrain structures. Also, the lack of NFIA and NFIB expression in callosally projecting neurons demonstrates that in corpus callosum development the principal function of these genes is to regulate development of midline glial structures that provide guidance for callosally projecting neurons.

## MATERIALS AND METHODS

### Animals

All procedures in this study were approved by the Animal Care and Use Committee at the University of Mary-

land, Baltimore, and the Animal Ethics Committee at the University of Queensland. Embryos and postnatal animals were obtained from timed-mated wildtype animals (C57Bl/6J mice, Jackson Labs, Bar Harbor, ME, or bred on site at the University of Queensland). Antibody specificity was examined using tissue from *Nfia* and *Nfib* knockout mice as previously described (das Neves et al., 1999; Shu et al., 2003; Steele-Perkins et al., 2005). GAD-67 animals were kindly provided by Dr. Yuchio Yanagawa (Gunma University Graduate School of Medicine, Maebashi, Japan) and were utilized to examine NFIA and NFIB expression in GABAergic interneurons. Embryonic day (E)0 refers to the day on which the presence of a vaginal plug was observed and the day of birth was designated as postnatal day (P)0. Tissue was collected from E11 to adult. To obtain embryonic brains, pregnant dams were anesthetized with an intraperitoneal injection of sodium pentobarbital (Nembutal; Abbott Laboratories, Abbott Park, IL). Embryos from E11 to E14 were immersion-fixed in 4% paraformaldehyde (PFA, prepared in 1× phosphate-buffered saline [PBS], pH 7.4). Embryos from E15 to E18 were perfused intracardially with saline solution (0.9% NaCl) followed by 4% PFA. Older animals (from P0 to adult) were deeply anesthetized with either ice (P0–5) or with sodium pentobarbital (P7-adult) and perfused intracardially with 0.9% saline followed by 4% PFA.

### Cortical cell culture

Cultures containing neurons and glia were prepared from C57Bl/6J cerebral cortex at E16. Briefly, cortices were dissected, trypsinized at 37°C for 5 minutes, and then triturated using an 18G needle. A cell count was performed where the number of dead cells were checked by Trypan-blue staining. Cells were plated at a density of  $4 \times 10^6$  cells/13 mm diameter on poly-D-lysine (50 µg/mL)-coated glass coverslips. Cells were grown for 7 days in vitro in DMEM with 10% fetal calf serum and B27 supplement (Invitrogen, La Jolla, CA). Cells were then washed in 1× PBS and fixed in 4% PFA for 15 minutes, after which they were processed for immunocytochemistry.

### Retrograde tracing

Postnatal C57Bl/6J mouse pups (age P1, P2, and P3) were anesthetized by hypothermia prior to microinjection. A small volume ( $\approx 1$  µL; 1 µg/µL) of true blue chloride (Invitrogen) retrograde tracer solution was drawn into the microneedle (diameter tip = 50–100 µm) connected to a micropipette holder, which in turn was attached to a mouse stereotaxic apparatus (Stoelting, Wood Dale, IL). A small incision was made in the scalp of the right hemisphere or in the dorsal skinfold between the shoulder blades up to the back of the neck over the pyramidal decussation at the base of the brain stem. The microneedle was lowered into the cortex (P1 or P3 for labeling of medial projections) or into the pyramidal decussation (P2 for lateral projections) with the aid of a micromanipulator pipette holder. The true blue retrograde tracer (0.5–1 µL) was then delivered by a picospritzer (Parker Instrumentation, Cleveland, OH; 30 ms duration, 20 psi) before removing the microneedle. The scalp/skin was sutured before returning the pup to its mother and littermates for overnight recovery. Pups were perfused intracardially (at P2 or P5 for cortical injections and at P3 for pyramidal decussation injected pups) as described and brains were

TABLE 1. Antibodies and Blocking Peptide Used for Western Blot and Immunohistochemistry Analysis

	GeneKa	Active motif	Isotype	Raised against	Dilutions
Antibodies					
NFIA	16111460	39329	Rabbit IgG	478-492 of human NF-1A	1/50K-1/75K
NFIB	16021117	39091	Rabbit IgG	402-415 of human NF-1B2	1/25K-1/50K
Peptides					
NFIA	N/A	N/A		N/A	N/A
NFIB	5021125	N/A		402-415 of human NF-1B2	1/500

processed for NFIA and NFIB immunohistochemistry (see below).

### Antibodies

NFIA and NFIB antibodies (Table 1) were made by GeneKa Biotechnology (Montreal, Canada) and later purchased from Active Motif (Carlsbad, CA). The rabbit polyclonal anti-NFIA antibody was raised against amino acids 478–492 of human NFIA (peptide sequence PSTSPANRFVSVGPR). The NFIA antibody was used at 1/75,000 for embryonic tissue and at 1/50,000 for postnatal tissue for Ni-DAB staining and at 1/1,000 for fluorescence. The rabbit polyclonal anti-NFIB antibody was raised against amino acids 402–415 of human NFIB (peptide sequence SPQDSSPRLSTFPQ) and used at 1/50,000 for embryonic tissue and at 1/25,000 for postnatal tissue when together with Ni-DAB and at 1/1,000 for fluorescence. The specificity of each antibody was analyzed using *Nfia* and *Nfib* knockout mice and by performing peptide blocking experiments (Fig. 1, Table 1). These control experiments confirmed the specificity of both antibodies.

The immunizing antigen for mouse anti-Tuj-1 (monoclonal; MAB1195; R&D Systems, Minneapolis, MN) was rat brain-derived microtubules. The specificity of this antibody has been demonstrated using Western blot analysis (Gass et al., 1990). In culture the Tuj-1 antibody stained cells with a neuronal morphology as previously demonstrated (Di Giorgi-Gerevini et al., 2005). Purified cell nuclei from mouse brain were used as the immunizing antigen to produce the mouse anti-NeuN antibody (monoclonal; MAB377; Clone A60; Chemicon, Temecula, CA). On a Western blot the antiserum recognizes two bands in the 46–48 kDa range (Chemicon technical information and Mullen et al. [1992]). Staining of sections through the forebrain produced a pattern of NeuN immunoreactivity that was identical to previous descriptions (Mullen et al., 1992; Wolf et al., 1996). Purified GFAP from porcine spinal cord was used as the immunizing antigen to produce the mouse anti-GFAP (monoclonal; MAB360; Clone GA5; Chemicon). On a Western blot the antiserum recognizes one band at 51 kDa (Chemicon technical information) and in culture only stained cells with the morphology of fibrillary astrocytes as previously demonstrated (Di Giorgi-Gerevini et al., 2005).

### Immunohistochemistry

After perfusion all tissues were postfixed in 4% PFA until use. Brains were blocked in 3% agar and cut at 40–50  $\mu\text{m}$  on a Vibratome (Leica, Deerfield, IL). Whenever possible, NFIA and NFIB immunohistochemistry were done on adjacent sections of the same brains for a better comparison of the protein expression. Sections were washed three times in 1 $\times$  PBS, blocked in a solution of 2% normal goat serum (v/v, S-1000, Vector Laboratories, Bur-

lingame, CA) and 0.2% Triton X-100 (v/v; Sigma, St. Louis, MO) in 1 $\times$  PBS for 2 hours. Sections were then incubated in primary antibodies (see antibodies section) at room temperature overnight. After three washes in 1 $\times$  PBS, sections were incubated in biotinylated goat antirabbit secondary antibody (BA-1000, 1/500, Vector Laboratories) for 1–2 hours at room temperature. Sections were then immersed in nickel-3,3'-diaminobenzidine (Ni-DAB) chromogen solution (2.5% nickel sulfate and 0.02% DAB in 0.175 M sodium acetate) activated with 0.01% (v/v) hydrogen peroxide until formation of a purple-to-black colored precipitate. The reaction was stopped with 1 $\times$  PBS and the sections were washed several times in 1 $\times$  PBS, after which they were mounted on gelatin-coated slides (0.5% gelatin) and dried overnight. Sections were then dehydrated through increasing ethanol concentrations, immersed in xylene, and coverslipped with D.P.X. mounting medium (Electron Microscopy Sciences, Fort Washington, PA). Sections for confocal fluorescence imaging were blocked as described, then incubated in primary antibody overnight at room temperature. Primary antibodies used were rabbit anti-NFIA or rabbit anti-NFIB (both used at 1/1,000; see below), and mouse anti-NeuN (1/1,000; Chemicon, MAB377). After three washes in 1 $\times$  PBS, sections were incubated for 2 hours at room temperature with fluorescent-conjugated secondary antibody (1/1,000, goat antirabbit AlexaFluor594, or goat antimouse AlexaFluor488, Invitrogen). DAPI (300 nM) was used as a counterstain and sections were mounted for fluorescence microscopy in PVA/DABCO (Fluka, Buchs, Switzerland). Immunocytochemistry on fixed, cultured cells was performed by first blocking and permeabilizing the cells in 1 $\times$  PBS containing 2% normal goat serum and 0.5% Triton X-100. Cells were incubated in primary antibodies for 2 hours at room temperature according to the following: rabbit anti-NFIA and rabbit anti-NFIB at 1/5,000; mouse anti-Tuj1 (R&D Systems, MAB1195) and mouse anti-GFAP (Chemicon, MAB360) at 1/1,000. Following washes in 1 $\times$  PBS the cells were incubated in the following secondary antibodies at 1/1,000 for 1 hour at room temperature: goat antimouse AlexaFluor488 or goat antirabbit AlexaFluor594 (Invitrogen). DAPI was used as a counterstain and the cells on coverslips were mounted for fluorescence microscopy as described.

### Western blot analysis

Cell extracts containing specific NFI proteins were prepared by transfection of JEG-3 choriocarcinoma cells with vectors expressing hemagglutinin (HA)-tagged NFIA, NFIB, NFI-C, and NFI-X as described previously (Chaudhry et al., 1997). Samples were lysed in 1 $\times$  SDS sample buffer, subjected to SDS-polyacrylamide gel electrophoresis, blotted to PVDF membranes, and detected using monoclonal antisera directed against the HA tag (C125A, Roche, Nutley, NJ) or

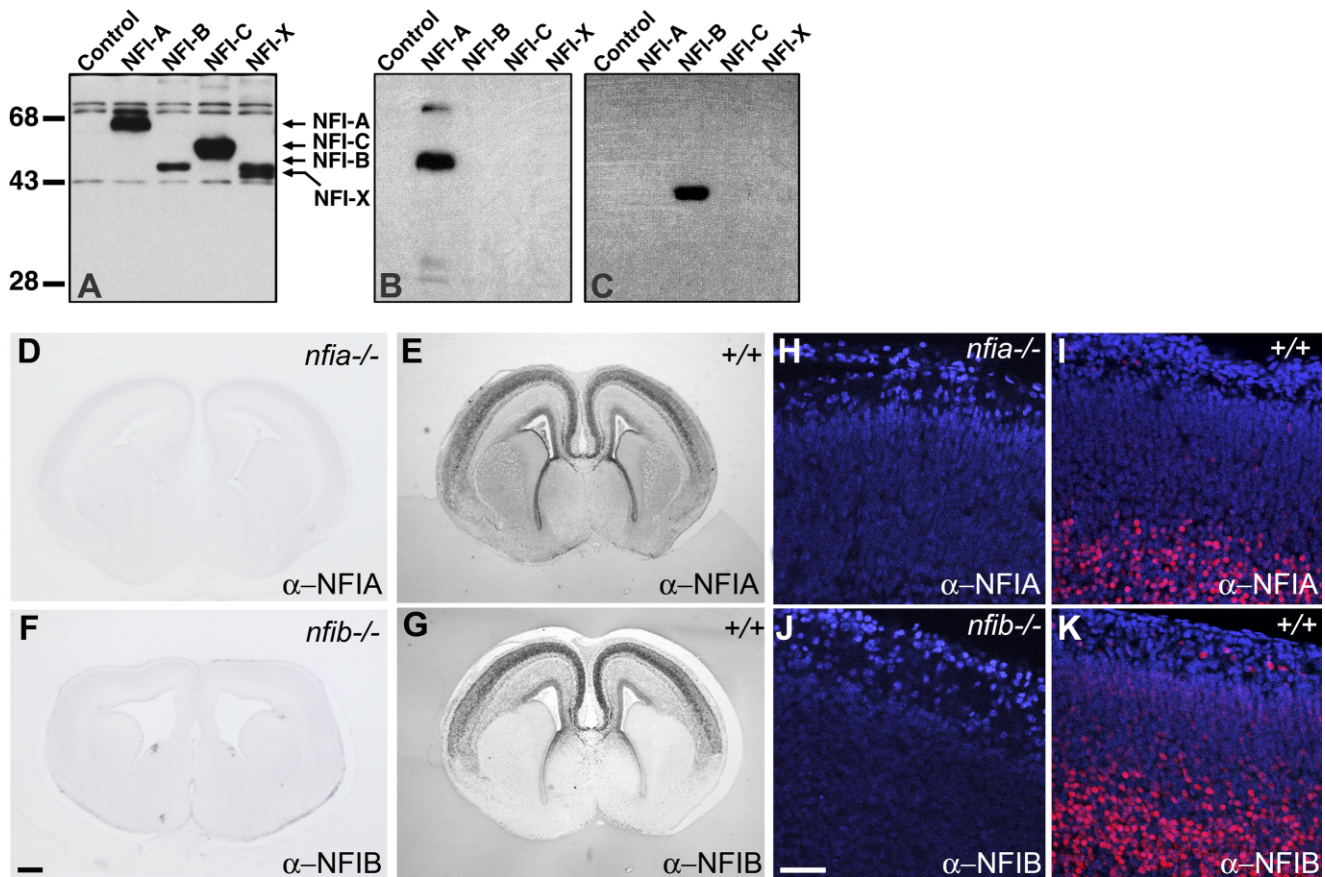


Fig. 1. Specificity of NFI antibodies. Extracts from control JEG-3 cells and cells transfected with vectors expressing the indicated NFI proteins were subjected to SDS-polyacrylamide gel electrophoresis and Western blot analysis using anti-hemagglutinin (HA) sera (A), an anti-NFIA antibody (B), and an anti-NFIB antibody (C). The bands obtained in each blot correspond to the appropriate molecular weight of the NFI proteins, respectively (HA-NFIA1.1, 57614 Da; HA-NFIB2, 49129 Da; HA-NFI-C2, 50425 Da; HA-NFI-X2, 46294 Da). The sizes of molecular weight standards are indicated on the left and the arrows in the center indicate the bands corresponding to HA-tagged NFIA, NFIB, NFI-C, and NFI-X. To test the specificity of the anti-NFIA and

NFIB antibodies we performed immunohistochemistry with a Ni-DAB chromogen on *Nfia* (D) or *Nfib* (F) knockout tissue and compared this to immunolabeling on wildtype sections (E,G, respectively). Since we also used these antibodies at a higher concentration for fluorescence, we tested their specificity using a fluorophore-conjugated secondary antibody (H-K). For fluorescent immunolabeling, DAPI was used as counterstain. In both cases, no labeling could be detected in any knockout tissue, indicating the specificity of each antibody. All sections shown are in the coronal plane. Scale bars = 500  $\mu$ m in F (applies to D-G); 100  $\mu$ m in J (applies to H-K).

antipeptide sera specific for NFIA or NFIB (39329 and 39091, respectively, Active Motif, Carlsbad, CA; see Table 1) followed by chemiluminescence (ECL) reagents (Amersham, Arlington Heights, IL).

### Image processing

Immunolabeling was analyzed with an upright light microscope (either Leica or Zeiss) and images were scanned with a digital camera (PhaseOne, Copenhagen, Denmark; or AxioCam HR, Zeiss). Fluorescent confocal microscopic images were obtained with a laser scanning microscope (Zeiss 510 META) microscope and software. All images were processed with Adobe Photoshop software (San Jose, CA).

## RESULTS

### Specificity of the NFI antibodies

To examine the specificity of the NFI antibodies used in this study we used Western blot analysis, immunoabsorp-

tion, and knockout tissue analysis (Fig. 1). For the Western blot analysis we used JEG-3 choriocarcinoma cells transfected with vectors expressing HA-tagged NFIA, NFIB, NFI-C, or NFI-X (Chaudhry et al., 1997). Each HA-tagged NFI factor was detected using an anti-HA antibody (Fig. 1A), and the band for each NFI protein was detected at its appropriate molecular weight. Similar blots, containing peptides of each of the four NFI family members, were immunostained with either the NFIA (Fig. 1B) or the NFIB (Fig. 1C) antibody. Each blot showed specific labeling of either the NFIA or NFIB lanes. Thus, these antibodies are specific for NFIA and NFIB and do not crossreact with other NFI family members. To further examine the antibody specificity we immunostained tissue from *Nfia* and *Nfib* knockout mice (das Neves et al., 1999; Steele-Perkins et al., 2005) using the NFIA and NFIB antibodies, respectively. No positive staining was detected in knockout brain sections for either the NFIA antibody (Fig. 1D,H, compared to wildtype tissue in Fig. 1E,I) or the NFIB antibody (Fig. 1F,J compared to wildtype tissue in

Fig. 1G,K). Finally, an NFIB blocking peptide, which had been used for immunizations when the antibody was made, was used in additional control experiments. Here the NFIB antibody was preabsorbed with the blocking peptide, after which no immunostaining was observed in sections (data not shown). No NFIA blocking peptide was available. From the control experiments we conclude that the NFIA and the NFIB antibodies specifically recognize the peptides they were designed against, and also that they do not give rise to any nonspecific background or crossreactivity with other NFI family members.

### Expression of NFI proteins in the developing telencephalon

The protein expression of NFIA and NFIB was analyzed in coronal and sagittal sections of developing mouse brain. In early telencephalic development (E12), immunostaining of coronal sections revealed that NFI proteins were expressed in the roofplate (Fig. 2A,B). NFIA or NFIB, however, were not expressed in cortical cells until after the formation of the preplate (Fig. 2C,C',D,D'). By E15, NFIA was expressed in layers IV, V, and VI, as well as in cells of the marginal zone and the subplate (Fig. 2E,E'). At this time, NFIB was expressed in layer VI, the subplate, and the marginal zone (Fig. 2F). By E17 both proteins were expressed in layer VI, the subplate, and the marginal zone. Essentially, the prenatal protein expression observed here confirms previous findings on mRNA expression of *Nfia* and *Nfib* in the developing telencephalon (Chaudhry et al., 1997), and protein expression of NFIA at E17 (Shu et al., 2003). At E18, NFIA and NFIB expression was also observed in the ventricular zone (VZ) and in the subventricular zone (SVZ), but at lower levels compared to in the neocortex. The expression of NFIA in the VZ and SVZ was found as early as E15 (Fig. 2E), E17 (Fig. 2G), and E18 (Fig. 2I,I'), whereas NFIB expression was observed in these proliferating regions at E17 (Fig. 2H) and at E18 (Fig. 2J,J').

In postnatal and adult brains, NFI proteins were expressed in specific layers in a dynamic manner. At P0, NFIA was highly expressed in layers II/III and V/VI, whereas NFIB expression was largely confined to layer IV (Fig. 3A,A',B,B'). At P7, NFIB was specifically expressed in layer VI (Fig. 3D,D'), while NFIA remained expressed in layers II/III and V/VI (Fig. 3C,C'). However, at this time NFIA expression began to decline, particularly in the upper layers. At P14, NFIA was specifically expressed in layer VI (Fig. 3E,E') in a similar, but delayed manner compared to the NFIB expression observed at P7. Both NFIA and NFIB expression then declined during postnatal cortex development (Fig. 3E–H,E'–H'). However, NFIA remained expressed in the piriform cortex at both P14 and in the adult (arrow in Fig. 3E,G), whereas NFIB was expressed in this area at P14 but not in the adult (arrow in Fig. 3F,H).

Sagittal sections were used to analyze the rostrocaudal distribution of NFI protein expression. Analysis of NFIA and NFIB protein expression in these sections matches the layer-specific expression observed in coronal sections (Fig. 4). In sagittal sections of prenatal brain (E13, E15, and E17) both NFIA and NFIB displayed a consistent level of distribution across the neocortex from rostral to caudal (Fig. 4A–F,A'–F'). However, in postnatal brains (P7 and P14) a lower level of NFIA protein was observed in rostral (Fig. 4G,G',I,I',I'') compared to caudal telencepha-

lon (Fig. 4G,G'',I,I''). No differences in the distribution of NFIB expression over the rostrocaudal axis was observed at these timepoints in deep layers of the cortex (Fig. 4H–H'', J–J'') but a graded expression was observed in layers II/III. The fact that higher levels of both NFIA and NFIB were observed in caudal compared to rostral telencephalon only at postnatal stages implies that this gene is not involved in early cortical arealization. However, graded expression of both these genes in postnatal stages may reflect either regionalized expression in all layers for NFIA or in layers II/III for NFIB. Still, this graded expression may also simply reflect the postnatal maturation of these telencephalic regions.

### Cell type-specific expression of NFI proteins

Dissociated E16 cortical cultures were utilized to assess whether NFIA and NFIB were expressed in neurons or glia (Fig. 5). Both proteins colocalized with both GFAP-positive glial cells (Fig. 5A,B) and with TuJ1-positive neurons (Fig. 5C,D). In these cultures, however, not all GFAP- and TuJ1-positive cells expressed NFIA or NFIB. DAPI staining confirmed the nuclear localization of both NFIA and NFIB (Fig. 5C,D). We also performed double labeling using P5 coronal sections and the neuronal marker NeuN together with either NFIA (Fig. 5E) or NFIB (Fig. 5F). In upper layers we found that NFIA did not colocalize with NeuN (arrows in Fig. 5E'), whereas in layer VI most NFIA-positive cells were NeuN-positive (arrowheads in Fig. 5E''). The majority of NFIB-positive cells throughout the cortical plate were NeuN-positive (arrowheads in Fig. 5F',F''). To investigate whether NFIA or NFIB were expressed in interneurons, we utilized the GAD67-GFP mouse, in which GABAergic neurons express GFP (Fig. 5G,H). We found that NFIA did not colocalize with GAD67-GFP in the marginal zone (Fig. 5G'), the cortical plate (Fig. 5G''), or in the dentate gyrus of the hippocampus (data not shown). Similar to NFIA, the majority of the NFIB-expressing cells did not express GAD67-GFP (Fig. 5H',H''), including cells in the dentate gyrus (not shown). However, a subpopulation of GAD67-GFP-expressing cells in the marginal zone (arrows in Fig. 5H') and a small number in the cortical plate (arrow in Fig. 5H'') were positive for NFIB.

Retrograde tracing was performed to analyze NFIA and NFIB expression in callosal (Fig. 6) and corticospinal (Fig. 7) projection neurons. The retrograde tracer true blue, when delivered into one cortical hemisphere at P1 or P3, retrogradely labeled callosally projecting neurons mainly in layer III of the contralateral hemisphere at P2 (data not shown) and at P5 (Fig. 6A,B, and higher magnification in A',B'), respectively. A small subpopulation of these projection neurons expressed NFIA (arrowhead in Fig. 6A'), but none expressed NFIB (Fig. 6B'). A few cells were true blue-positive in deeper layers of the cortex at P5 (Fig. 6A'',B''), but none of these cells were positive for either NFIA or NFIB. When delivered into the pyramidal decussation at P2, true blue retrogradely labeled lateral projecting neurons of layer V in both hemispheres at P3 (Fig. 7A,B). The majority of these true blue-positive cells expressed NFIA (arrowheads in Fig. 7A') and NFIB (arrowheads in Fig. 7B'). Taken together, neither NFIA nor NFIB is expressed in the majority of neurons projecting across the midline through the corpus callosum. Most

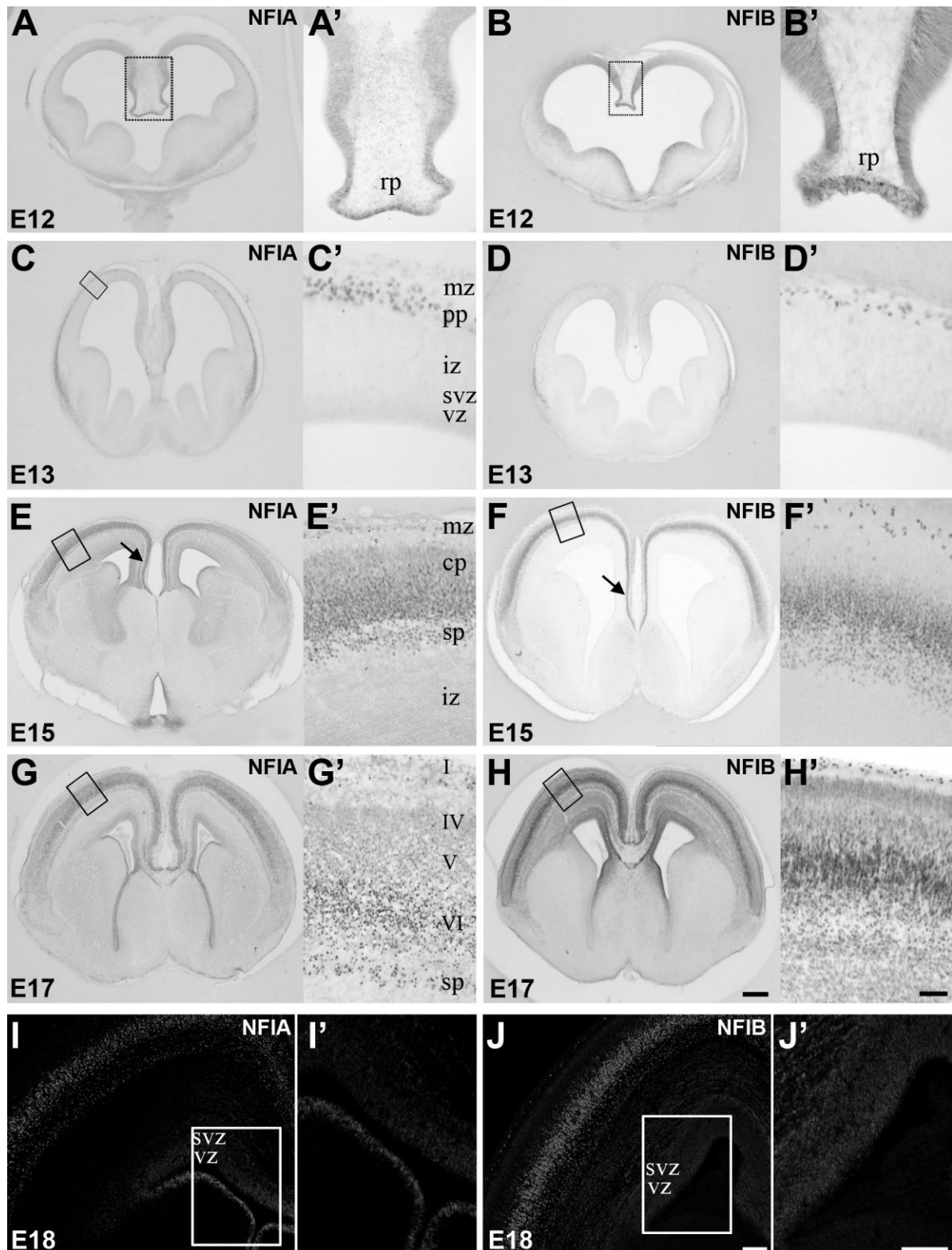


**Fig. 2.** NFI protein expression in embryonic dorsal telencephalon. We examined the expression of NFIA and NFIB proteins in coronal sections during the development of embryonic dorsal telencephalon. NFIA and NFIB proteins were detected in the roof plate (rp) at E12 (**A**, and higher magnification in **A'** for NFIA; **B**, and higher magnification in **B'** for NFIB). At E13, both proteins were expressed in the preplate and marginal zone (pp, mz, **C,C'** and **D,D'**). At E15, NFIA was expressed throughout the cortical plate and in the marginal zone (mz, **E,E'**), whereas NFIB became restricted to the deeper layers of the cortex and a few cells in the subplate (sp) and the marginal zone (**F,F'**). At E15, both NFIA and NFIB were also expressed in the cingulate cortex (arrows in **E,F**). At E17, NFIA expression was lower

in the upper cortical layers, but high in layer VI and the subplate (**G,G'**). NFIB expression remained high in the deep cortical layers, marginal zone, and subplate. NFIA and NFIB expression was also observed at low levels in the VZ and in the SVZ (at E15 for NFIA only, **E**), at E17 (**G,H**) and E18 (**I,I',J,J'**). cp, cortical plate; iz, intermediate zone; mz, marginal zone; pp, preplate; rp, roof plate; sp, subplate; svz, subventricular zone; vz, ventricular zone; I, IV, V, VI, cortical layers. Scale bars = 600  $\mu$ m in H for A–D; 520  $\mu$ m for E,F; 480  $\mu$ m for G,H; 150  $\mu$ m in H' for A',B'; 80  $\mu$ m for C',D'; 50  $\mu$ m for E'–H'; 100  $\mu$ m in J,J' for I–J'. [Color figure can be viewed in the online issue, which is available at [www.interscience.wiley.com](http://www.interscience.wiley.com).]

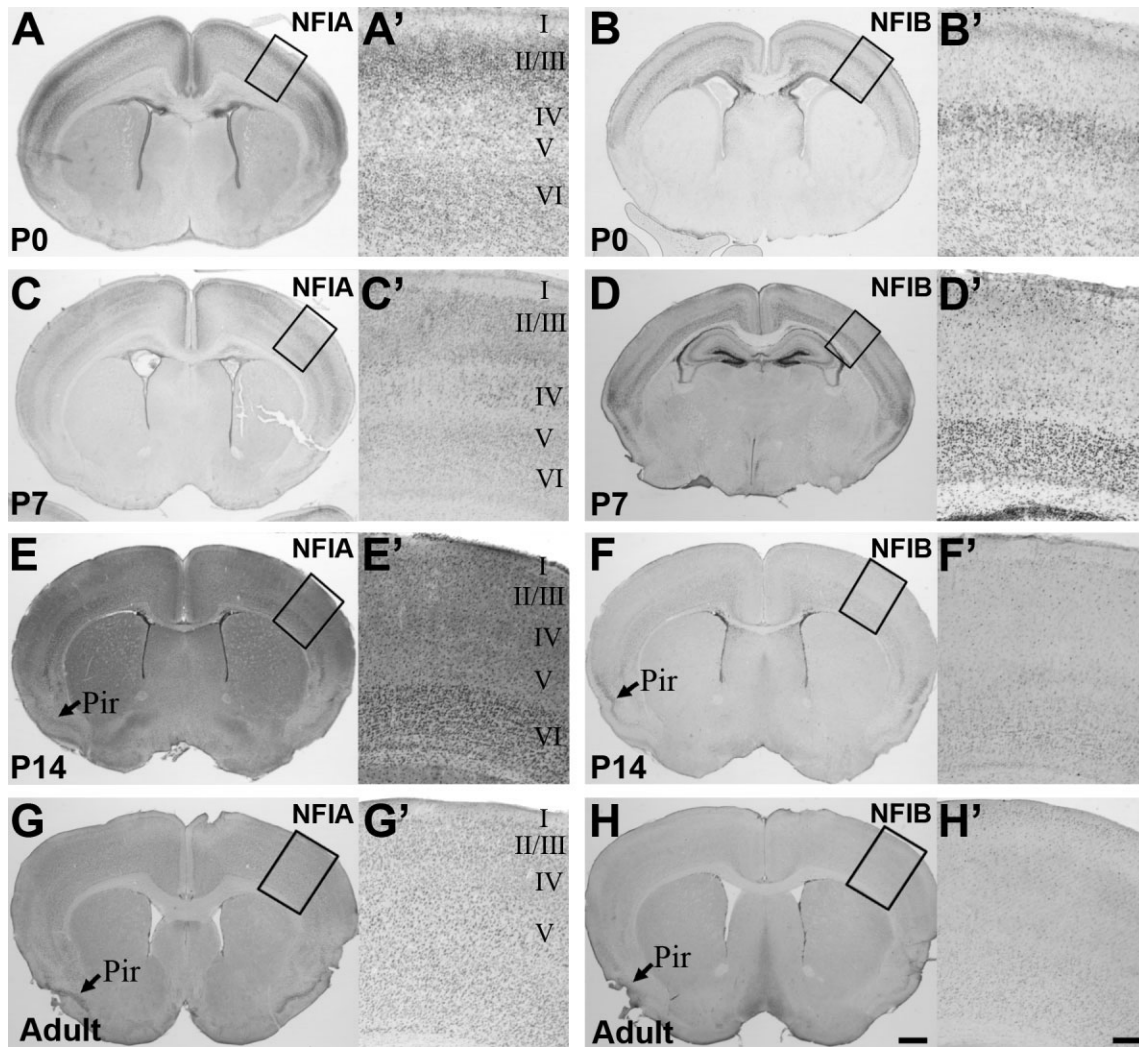


Fig. 3. Dynamic NFI expression in the postnatal mouse cerebral cortex. The expression of NFIA and NFIB proteins were examined in coronal sections of mouse cerebral cortex from P0 to adult. The expression pattern of the two genes was dynamic and differed during this period. At P0, NFIA was expressed throughout the cortical plate but higher expression levels were detected in layers II/III and in deeper layers (A, higher magnification of the cortical layers in A'). NFIB, on the other hand, was specifically expressed in layer IV (B and higher magnification in B'). At P7, NFIA was expressed more uni-

formly throughout the cortical layers (C,C'). NFIB expression was highest in layer VI (D,D'). At P14, NFIA expression was observed in layer VI (E,E'), whereas NFIB expression was observed throughout the cortical layers (F,F'). At this stage and in the adult, NFIA and NFIB were also expressed in the piriform cortex (Pir, E-G). In the adult the expression of both proteins declined (G,G' and H,H'). Pir, piriform cortex; I, IV, V, VI, cortical layers. Scale bars = 400  $\mu$ m in H for A,B; 625  $\mu$ m for C-H; 200  $\mu$ m in H' for A',B'; 100  $\mu$ m for C',D'; 250  $\mu$ m for E'-H'.

layer V neurons projecting laterally, however, express both NFIA and NFIB.

#### NFI expression at the midline of the developing cerebral cortex

Four midline populations are positioned at the cortico-septal boundary: the GW (Shu and Richards, 2001), the IGG, the midline zipper glia (MG) (Silver et al., 1993), and the SS (Silver et al., 1982; Shu et al., 2003). At E15, NFIA and NFIB protein was detected in the cingulate cortex (Fig. 8A,B), but only NFIA was expressed in midline glial populations (Fig. 8A) at this time. We previously demonstrated that NFIA in fact colocalizes with GFAP in both the GW and the IGG at E17 (Shu et al., 2003). NFIB

expression had increased by E18, and both NFIA and NFIB were observed in the midline in regions overlapping the location of all midline glial populations (Fig. 8C,D). During postnatal development, NFI proteins were still detected at the midline and also lining the ventricles (Fig. 8G,H). In the adult, cells within the subventricular zone expressed both NFIA and NFIB (Fig. 8I,J) and both proteins were expressed in nonoverlapping populations within the IGG (Fig. 8I',J').

#### Expression of NFI proteins in thalamus and ventral telencephalon

As early as E12, weak NFIA labeling was detected in the posterior thalamus, hypothalamus, and optic chiasm

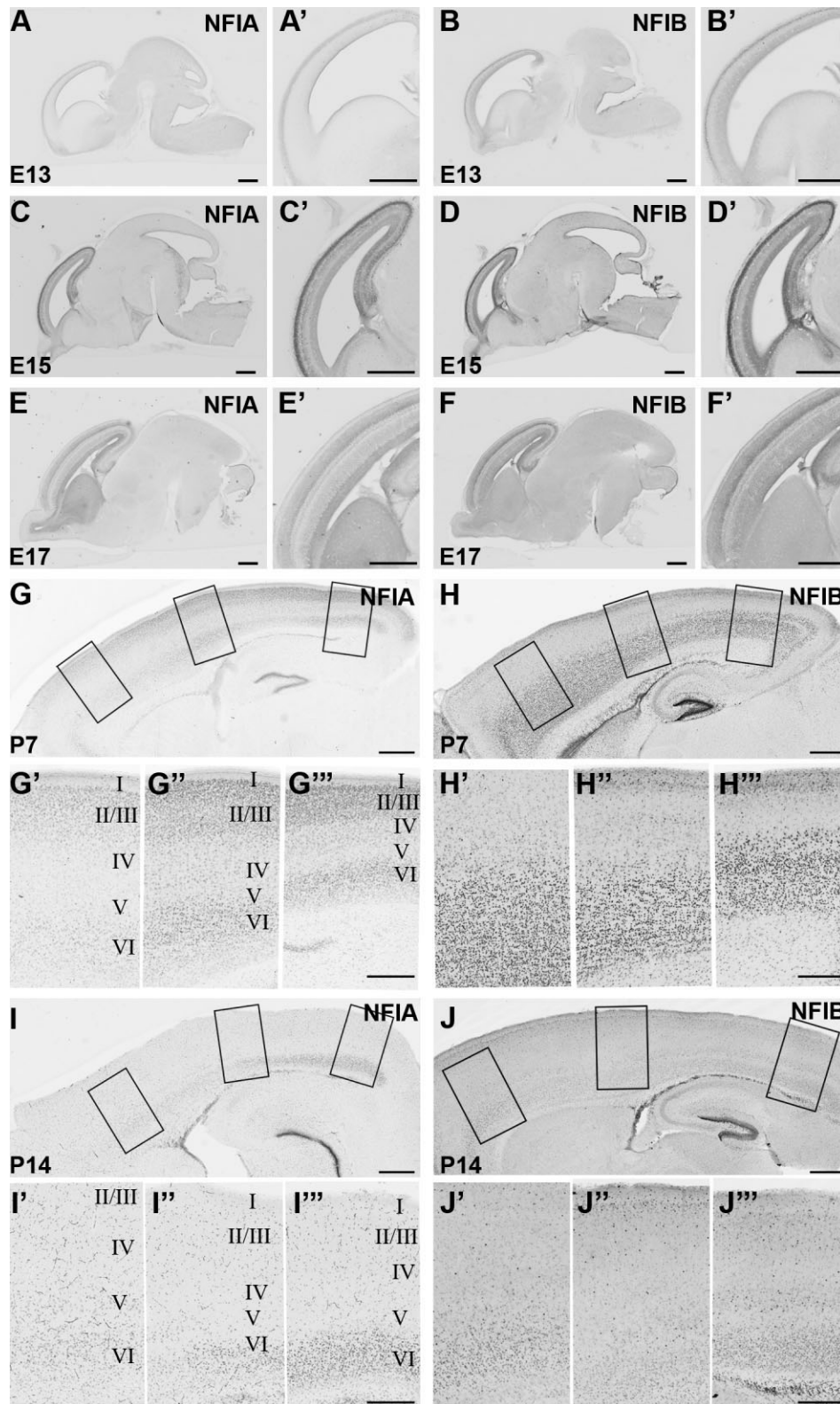


Fig. 4. Rostrocaudal distribution of NFIA and NFIB expression. The protein expression of NFIA and NFIB was analyzed in sagittal sections of pre- and postnatal mouse brain. In prenatal telencephalon (E13, E15, and E17) an even neocortical expression along the rostrocaudal axis was observed for both NFIA (A,A',C,C',E,E') and NFIB (B,B',D,D',F,F'). In postnatal telencephalon, NFIA was expressed at lower levels in rostral compared to caudal neocortex (P7, G; higher magnification of the three boxed regions in G', rostral; G'', middle; and G''', caudal neocortex, and P14, I; higher magnification of the three boxed regions in I', rostral; I'', middle; and I''', caudal neocor-

tex). No differences in the levels of NFIB expression could be detected over the rostrocaudal neocortical axis at P7 (H; higher magnifications of the boxed regions from rostral to caudal in H', H'', and H''', respectively). However, changes in levels of NFIB expression in layers II/III were detected over the rostrocaudal neocortical axis at P14 (P14, J; higher magnification of the three boxed regions in J', rostral; J'', middle; and J''', caudal neocortex). Cortical layers are delineated by I, II/III, IV, V, and VI. Scale bars = 500  $\mu$ m in F for A-F; 100  $\mu$ m in F' for panels A'-F'; 500  $\mu$ m in J for G-J; 100  $\mu$ m in J''' for G'-J'''.

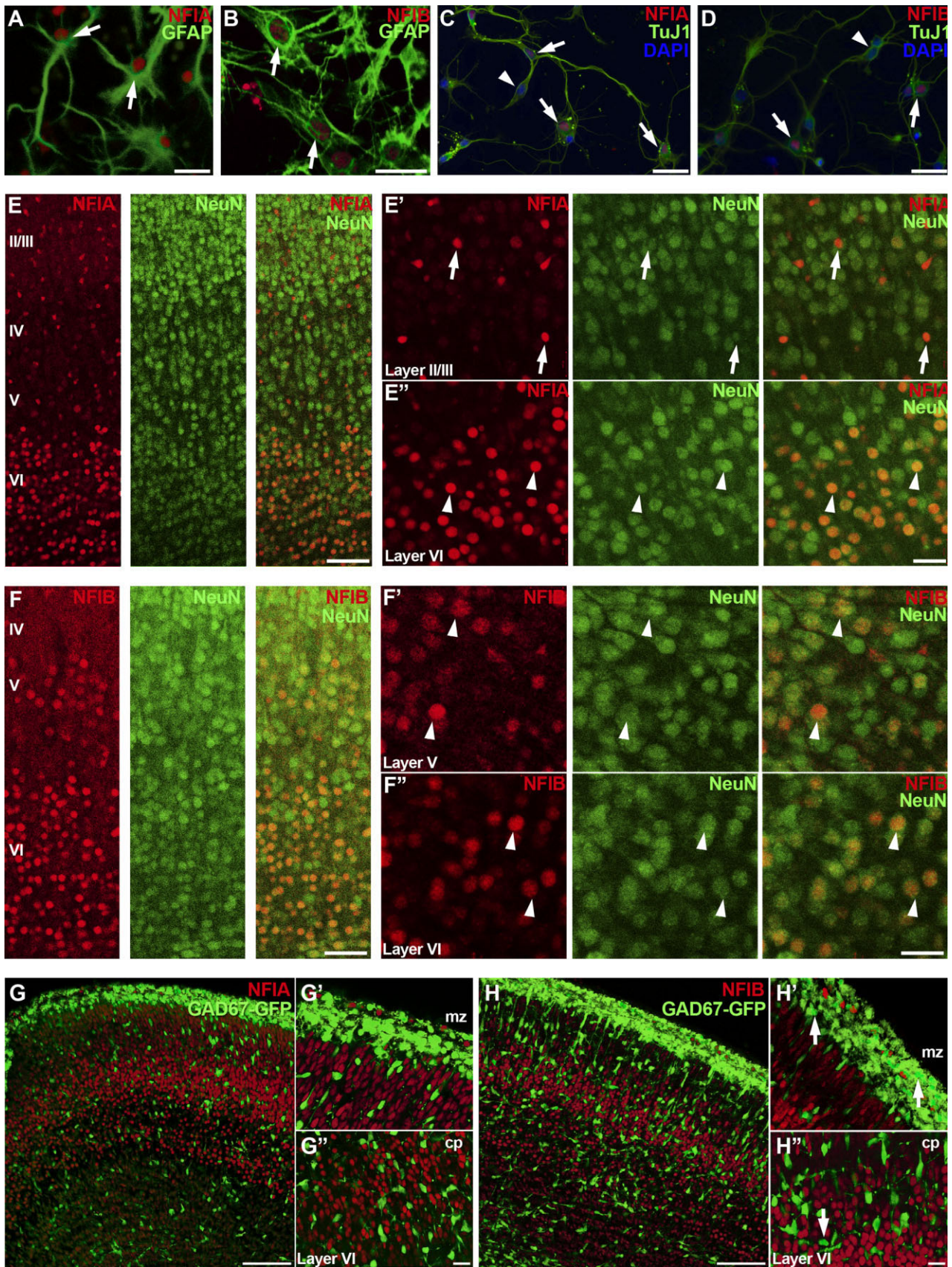


Figure 5

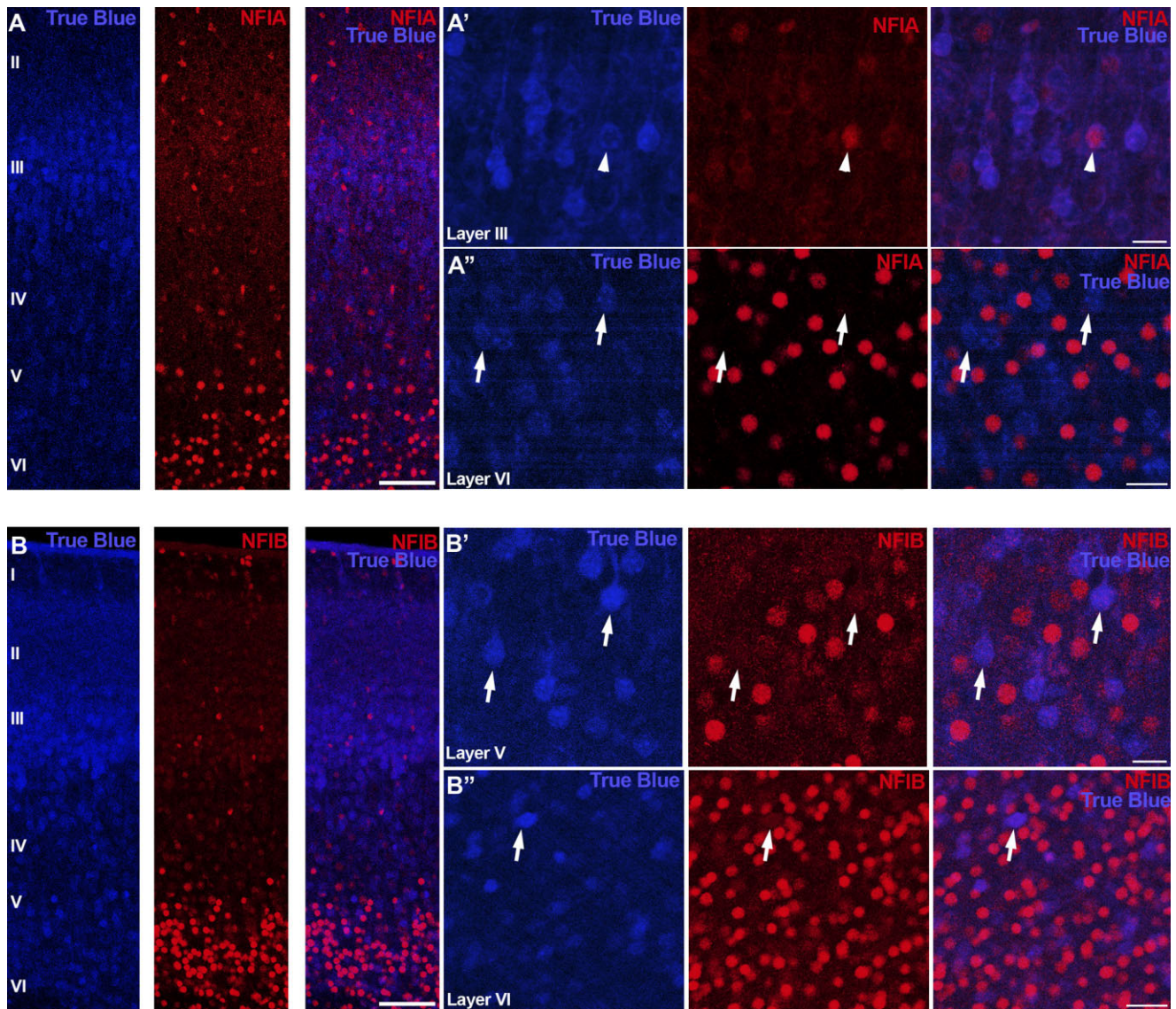


Fig. 6. NFI expression in neurons projecting across the midline through the corpus callosum. The retrograde tracer true blue was injected into one hemisphere of cortex at P3 to label contralaterally projecting neurons. Brains were then fixed at P5. True blue-positive cells were observed mainly in layer III and in lower numbers in deeper layers. Coronal sections were analyzed at P5 for NFIA (A–A'') and NFIB (B–B'') expression, respectively. In layer III a small subpopu-

lation of true blue positive cells were NFIA positive (arrowhead in A'), whereas no double-labeled cells were found in deeper layers (arrows in A''). NFIB was not observed in any true blue-positive cells throughout the cortex (higher magnification of layers V and VI in B' and B'', with arrows pointing to true blue-positive cells). Cortical layers are delineated by I, II/III, IV, V, and VI. Scale bars = 100  $\mu\text{m}$  for A,B; 20  $\mu\text{m}$  for A'–B''.

Fig. 5. Cell type-specific expression of NFIA and NFIB. Cell type-specific expression of NFIA and NFIB was examined in dissociated cortical cultures (A–D) as well as in coronal sections of either wildtype (E–F'') or GAD67-GFP brains (G–H''). Dissociated cortical cultures were double-labeled with either glial-specific GFAP (A,B), or neuron-specific TuJ1 (C,D) antibodies, together with either NFIA or NFIB. NFI expression was observed in both neurons and glial cells (arrows) but not all TuJ1+ cells expressed NFIA or NFIB (arrowheads). DAPI was used as a counterstain, which revealed the nuclear localization of both NFIA (C) and NFIB (D). Coronal sections of P5 brains were labeled with the neuronal marker NeuN together with either NFIA (E) or NFIB (F). NFIA-positive cells were observed in layer VI and scattered throughout layer II–V. NFIA did not colocalize with NeuN

in upper layers (arrows in E'), whereas in layer VI the majority of the NFIA-positive nuclei were NeuN-positive (arrowheads in E''). NFIB-positive nuclei were observed in layers V and VI (F), and the majority of these colocalized with NeuN positive nuclei (arrowheads, in F',F''). E18 GAD67-GFP brains were utilized for analysis of NFI expression in GABAergic interneurons (G,H). No colocalization of NFIA with GAD67-GFP-positive cells was observed (G–G''). The majority of NFIB-positive cells also did not colocalize with GAD67-GFP, but a small subpopulation of cells in the marginal zone and a few cells in the cortical plate expressed both GAD67-GFP and NFIB (arrows in H',H''). Cortical layers are delineated by I, II/III, IV, V, and VI; cp, cortical plate; mz, marginal zone. Scale bars = 20  $\mu\text{m}$  for A–D; 50  $\mu\text{m}$  for E,F; 20  $\mu\text{m}$  for E'–F'': 100  $\mu\text{m}$  for G,H; 10  $\mu\text{m}$  for G'–H''.

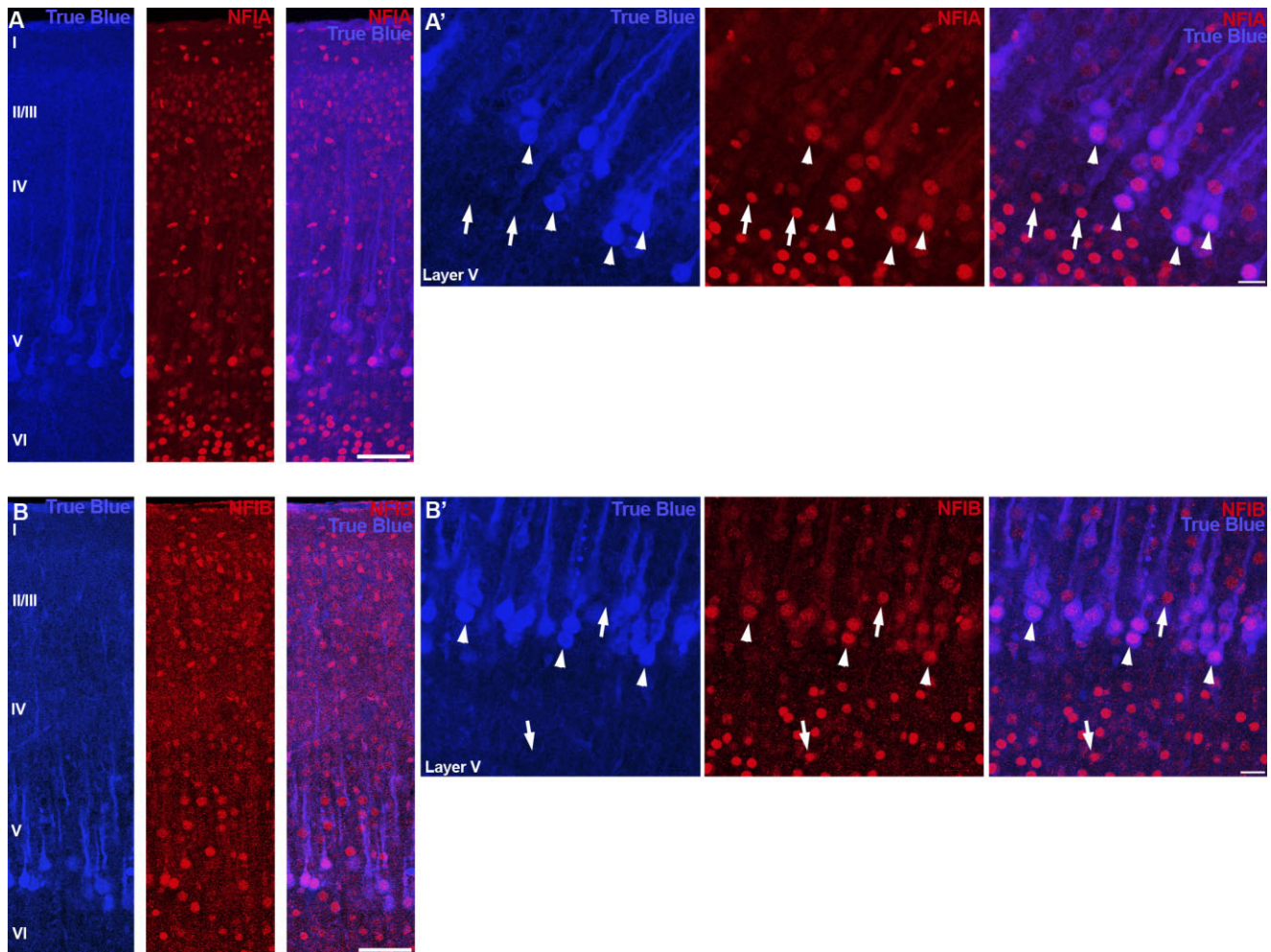


Fig. 7. NFI expression in laterally projecting neurons. The retrograde tracer true blue was injected into the pyramidal decussation of P2 mice and NFIA and NFIB expression was analyzed in fixed coronal sections at P3. True blue-positive cells were observed only in layer V, and the majority of these cells were colabeled with NFIA (A, and

arrowheads in A') and NFIB (B, and arrowheads in B'). Arrows in A' and B' point to cells in layer VI, which are not double-labeled with true blue and either of NFIA and NFIB, respectively. I, II, III, IV, V and VI, cortical layers. Scale bars = 100  $\mu$ m for A,B; 20  $\mu$ m for A',B'.

(Fig. 9A,A',C,C'). A similar pattern of expression was observed for NFIB, except no expression was detected in the optic chiasm at this timepoint (Fig. 9B,B',D,D'). At E12 and E13, NFIA was also expressed in the amygdala (Fig. 9A,C, respectively) where it continued to be expressed at E13 (Fig. 9C). At E18, cells expressing NFIA and NFIB were observed in the hypothalamus (Fig. 9E,E',F,F') and in cells lining the third ventricle (Fig. 9E',F'). At P2, NFIB expression could no longer be detected in the thalamus (data not shown), whereas at P5, NFIA was expressed in the dorsal thalamus (Fig. 11A), but disappeared by P7 (Fig. 11C).

### NFI proteins are dynamically expressed in specific hippocampal cell populations

Around E12/E13 in mouse the neuroepithelium in the dorsomedial wall of the telencephalon begins to protrude into the lateral ventricle to form the future hippocampus (Bayer, 1980). NFI proteins were detected in this area as soon as the hippocampal primordium appeared (Fig.

10A,A',B,B'). By E15 the distinct layers of the hippocampus appeared, expressing NFIA throughout (Fig. 10C,C'), whereas NFIB expression was highest in the hippocampal stratum radiatum (sr, Fig. 10D,D'). At E17 the dentate gyrus expressed both NFIA and NFIB (Fig. 10E,E',F,F'). Expression in the stratum radiatum ceased by E17 for both proteins. At this time NFIB expression was most apparent in the stratum oriens (Fig. 10F,F'), whereas NFIA expression was observed in both the stratum oriens and the stratum pyramidale (Fig. 10E,E'). In the first postnatal week the hippocampal Cornu Ammons (CA) areas 1–3 and the dentate gyrus were positive for NFIA (Fig. 11A–A'''), whereas NFIB labeled the dentate gyrus specifically (Fig. 11B–B'''). At P5, NFIA expression was also observed in the stratum pyramidale (Fig. 11A'). Both NFIA and NFIB strongly labeled the dentate gyrus throughout development and into adulthood (Fig. 11). Outside the dentate gyrus, NFIA was expressed in a dynamic manner in the CA regions. At P5, NFIA expression was higher in CA3 than in CA2, and expression in CA2

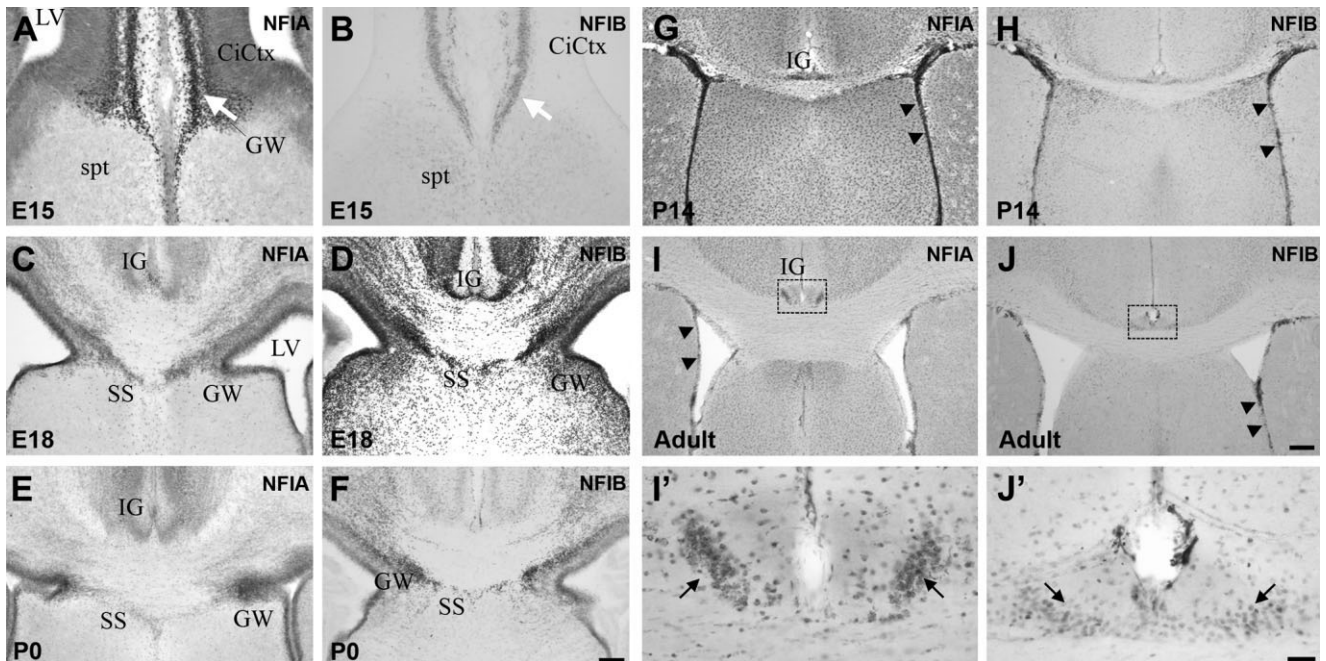


Fig. 8. NFI expression at the midline of the cerebral cortex. NFIA and NFIB protein expression was investigated at the midline in coronal sections from E15 to adult. At E15 both NFIA and NFIB were strongly expressed in the cingulate cortex (white arrow in **A,B**, respectively). NFIA was more widely expressed throughout the ventricular zone and in cells of the indusium griseum and the glial wedge (**A**) compared to NFIB (**B**). At E18 (NFIA in **C**, NFIB in **D**) and P0 (NFIA in **E**, NFIB in **F**), both NFIA and NFIB proteins were detected in the indusium griseum, the glial wedge, and also in the subcallosal sling. At P14, NFIA expression at the midline was higher than NFIB expression (**G** compared to **H**). Both genes were expressed in the ven-

tricular zone/ependymal layer at P14 and in the adult (arrowheads in **G,H**, and **I,J**, respectively). **I,J'** are higher magnifications of the boxed regions in **I,J**, respectively, and demonstrate the expression of both genes in the indusium griseum of the adult. Different NFIA- and NFIB-positive populations were observed in the indusium griseum, where NFIA-positive cells (arrows in **I'**) were present more dorsomedially than the NFIB-expressing cells (arrows in Panel **J'**). All sections shown are in the coronal plane. IG, indusium griseum; GW, glial wedge; SS, subcallosal sling; CiCtx, cingulate cortex; LV, lateral ventricle. Scale bars = 70  $\mu$ m in **F** for **A,B**; 100  $\mu$ m for **C-F**; 200  $\mu$ m in **J** for panels **G-J**; 30  $\mu$ m in **J'** for **I',J'**.

was higher than in CA1 (Fig. 11A", CA3>CA2>CA1). At P7 and P14, NFIA expression increased in CA1, whereas a decrease was observed in CA2 and CA3 (Fig. 11C',E'). In the adult, NFIA was weakly expressed throughout the hippocampus (Fig. 11G–G"), except from some residual cells that were NFIA-positive in the inner granule layer of the dentate gyrus (Fig. 11G"). NFIA expression was low but still present in CA3 (Fig. 11G"), whereas low NFIB expression was detected in CA2 (Fig. 11H"). NFIB was predominantly expressed in the dentate gyrus throughout hippocampal development, and its expression remained high in the adult, especially in the granule layer (Fig. 11H").

## DISCUSSION

The dynamic expression of NFIA and NFIB observed in various telencephalic structures, and in different layers of the developing cortex and hippocampus, indicate that these genes could play roles in numerous developmental processes. It is likely that such roles depend not only on which cells express NFIA and NFIB, but also on the spatial expression of NFI proteins, for example through possible dimer combinations (Kruse and Sippel, 1994), and on their temporal expression, where NFIA and NFIB could regulate developmental processes according to input from the changing environment. In addition, the expression of

NFIA and NFIB in both glial structures and neurons suggests that the role of these proteins in formation of forebrain neural networks could be a combination of cell-autonomous and nonautonomous developmental processes.

### NFI protein expression in the developing cortex

During early telencephalic development, NFIA and NFIB are both expressed in the roofplate, an epithelial layer involved in dividing the telencephalon into the two cortical hemispheres. This structure has been suggested to constitute an organizing center, regulating the early transformation and patterning of the dorsal telencephalon (Monuki et al., 2001; Cheng et al., 2006). Various molecules are involved in the roof plate-mediated patterning of the cerebral cortex, including *Bmp2*, *Bmp4*, and *Lhx2* (Monuki et al., 2001; Cheng et al., 2006). The role of NFI proteins in developmental patterning, however, is still unclear, but their expression in these regions suggests that they may be involved in patterning the dorsal telencephalon and/or the formation of the roof plate. Interestingly, in addition to its role in roof plate-mediated patterning, *Lhx2* has previously been shown to be important for formation of midline glia in zebrafish, and like the *Nfia* and *Nfib* knockout mouse phenotypes, *Lhx2* deficiency in zebrafish also leads to a failure of commissural axons to

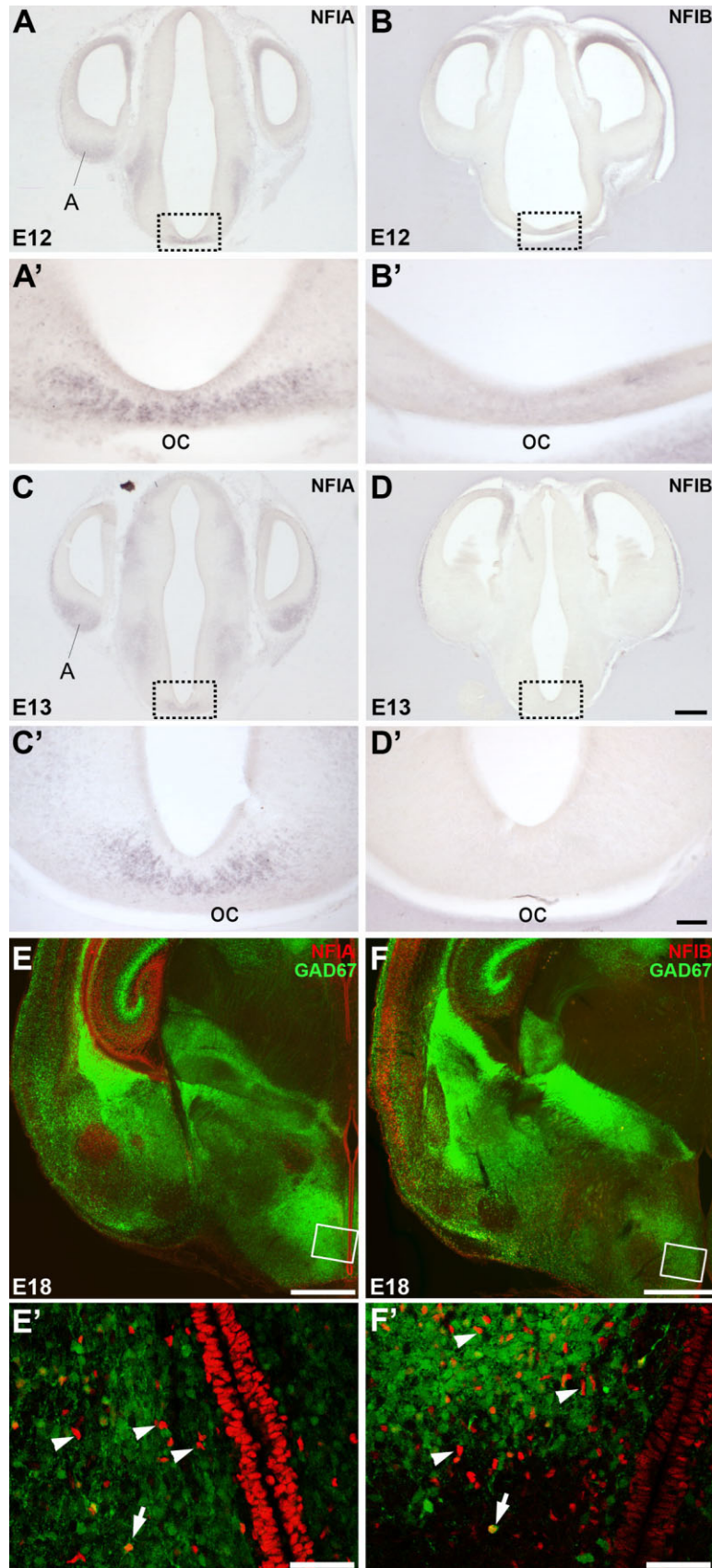


Fig. 9. NFI expression in the ventral thalamus and ventral telencephalon. NFIA and NFIB were expressed in the ventral thalamus at E12 (**A,B**, respectively) and E13 (**C,D**, respectively), but only NFIA was expressed in the region of the developing optic chiasm at E12 (**A,A'** higher magnification of the box in **A**) and at E13 (**C,C'**). As shown in **B',D'** (higher magnification of **B,D**, respectively), no NFIB proteins were detected in the optic chiasm at those stages. NFIA proteins were also observed in the amygdala at E12 (**A**) and E13 (**C**). No NFIB expression was detected in the amygdala. At E18, cells

expressing NFIA and NFIB were found scattered within the ventral thalamus (**E,F**, respectively, and higher magnification of the boxes in **E',F'**). A small number of these cells were double-labeled with GAD67-GFP (arrows in **E',F'**), whereas most were not (arrowheads). Also, note the NFIA- and NFIB-positive cells lining the third ventricle (**E',F'**). All sections shown are in the coronal plane. A, amygdala; oc, optic chiasm. Scale bars = 300  $\mu$ m in **D** for panels **A-D**; 45  $\mu$ m in **D'** for **A',B'**; 60  $\mu$ m for **C',D'**; 500  $\mu$ m for **E,F**; 40  $\mu$ m for **E',F'**.

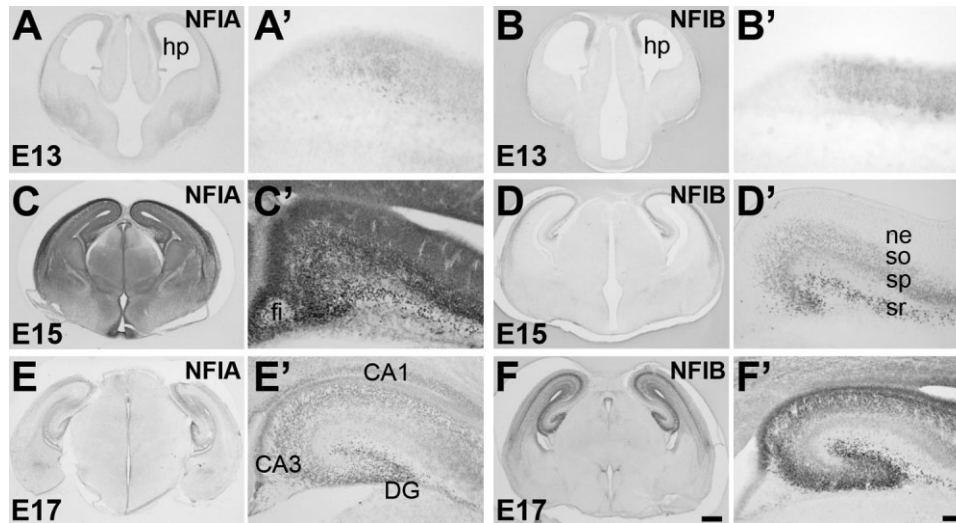


Fig. 10. NFI protein expression in the developing hippocampus. NFIA and NFIB proteins were expressed as soon as the hippocampal primordium developed (NFIA in **A**, and higher magnification in **A'** and NFIB in **B**, and higher magnification **B'**). By E15, NFIA was expressed throughout the hippocampal primordium in both the ventricular zone and differentiating cells that have migrated to form the stratum radiatum and the stratum pyramidale (**C,C'**). NFIB expression however is confined to the differentiating cells of these layers (**D,D'**). By E17 both NFIA and NFIB were expressed throughout all

differentiating fields of the hippocampus although NFIB appeared more strongly expressed than NFIA, particularly in the dentate gyrus (**F**, and high power view in **F'**). All sections shown are in the coronal plane. hp, hippocampal primordium; fi, fimbria; ne, neuroepithelium; so, stratum oriens; sp, stratum pyramidale; sr, stratum radiatum; DG, dentate gyrus; CA, Ammon's horn. Scale bars = 270  $\mu$ m in **F** for **A,B**; 360  $\mu$ m for **C,D**; 400  $\mu$ m for **E,F**; 60  $\mu$ m in **F'** for **A'-D'**; 90  $\mu$ m for **E',F'**.

cross the midline (Seth et al., 2006), suggesting potential common genetic pathways. However, identifying and clarifying the role of NFI upstream candidates such as *Emx2*, *Pax6*, and *Neurogenin2* (Mattar et al., 2004; Gangemi et al., 2006; Holm et al., 2007), as well as downstream effectors of NFI proteins, will prove pivotal in understanding how they may affect the molecular pathways involved in early telencephalic patterning.

The transcription factors *Emx2* and *Pax6*, both possible upstream effectors of the *Nfi* genes (Gangemi et al., 2006; Holm et al., 2007), are involved in regulating the developmental arealization of the cortex (Bishop et al., 2000; Mallamaci et al., 2000). *Emx2* and *Pax6* are expressed in complementary gradients across the developing embryonic neocortex. *Emx2* is expressed in a low rostral to high caudomedial gradient (Mallamaci et al., 1998), whereas *Pax6* is expressed in a high rostral to low caudomedial gradient (Stoykova and Gruss, 1994). Given the graded expression of *Emx2* and *Pax6*, and that NFI proteins may be downstream targets of these genes, we reasoned that the *Nfi* genes may also be expressed in a developmental gradient. To investigate this, we analyzed NFIA and NFIB immunolabeling in sagittal sections of the developing telencephalon. However, we did not detect a prenatal graded expression of either protein across the rostrocaudal axis of the neocortex. Postnatally, however, NFIA cortical expression as well as NFIB expression in layers II/III showed a low rostral to high caudal gradient across the neocortex. Nevertheless, a true developmental expression gradient would have been consistent over time and, thus, we conclude that the observed NFIA expression gradient rather represents cells at different stages of development across the rostrocaudal axis of the neocortex. Taken together, our findings suggest that neither NFIA

nor NFIB are involved in the early patterning of the neocortex into different sensory and motor regions, as has been shown for *Emx2* and *Pax6* (Bishop et al., 2000; Mallamaci et al., 2000).

The earliest born cortical neurons in the developing telencephalon form the preplate, a layer of differentiated neurons superficial to the proliferative zones. The subsequent wave of migrating cortical cells splits the preplate into two layers: a superficial marginal zone and a deeper subplate (Luskin and Shatz, 1985; Marin-Padilla, 1998). NFIA and NFIB are first expressed in the differentiating cells of the preplate. Later, however, expression was also observed in the proliferative zones of the cortex (the VZ and the SVZ), although at lower levels compared to expression in the cortical plate. The preplate is important for development of the radial glial scaffold, and is thus crucial for the radial migration of cortical neurons (Xie et al., 2002). In transgenic mice, where preplate cells have been ablated, radial glia are malformed and also reduced in numbers. This deficit subsequently caused impaired radial migration of cortical projection neurons (Xie et al., 2002). The expression of NFI proteins in the preplate indicates that they could be involved in regulating processes early in cortical development, but their precise roles are unclear.

In mouse, callosal axons extend predominantly from cortical layers II/III and V. After E15, when the first axons of the corpus callosum have crossed the midline, NFIA is expressed throughout the cortical plate, whereas NFIB expression is confined to deeper layers. Both *Nfia*- and *Nfib*-deficient mice display agenesis of the corpus callosum (Shu et al., 2003; Steele-Perkins et al., 2005), and this abnormality prompted us to investigate whether cortical NFIA and NFIB expression could be involved in cell-

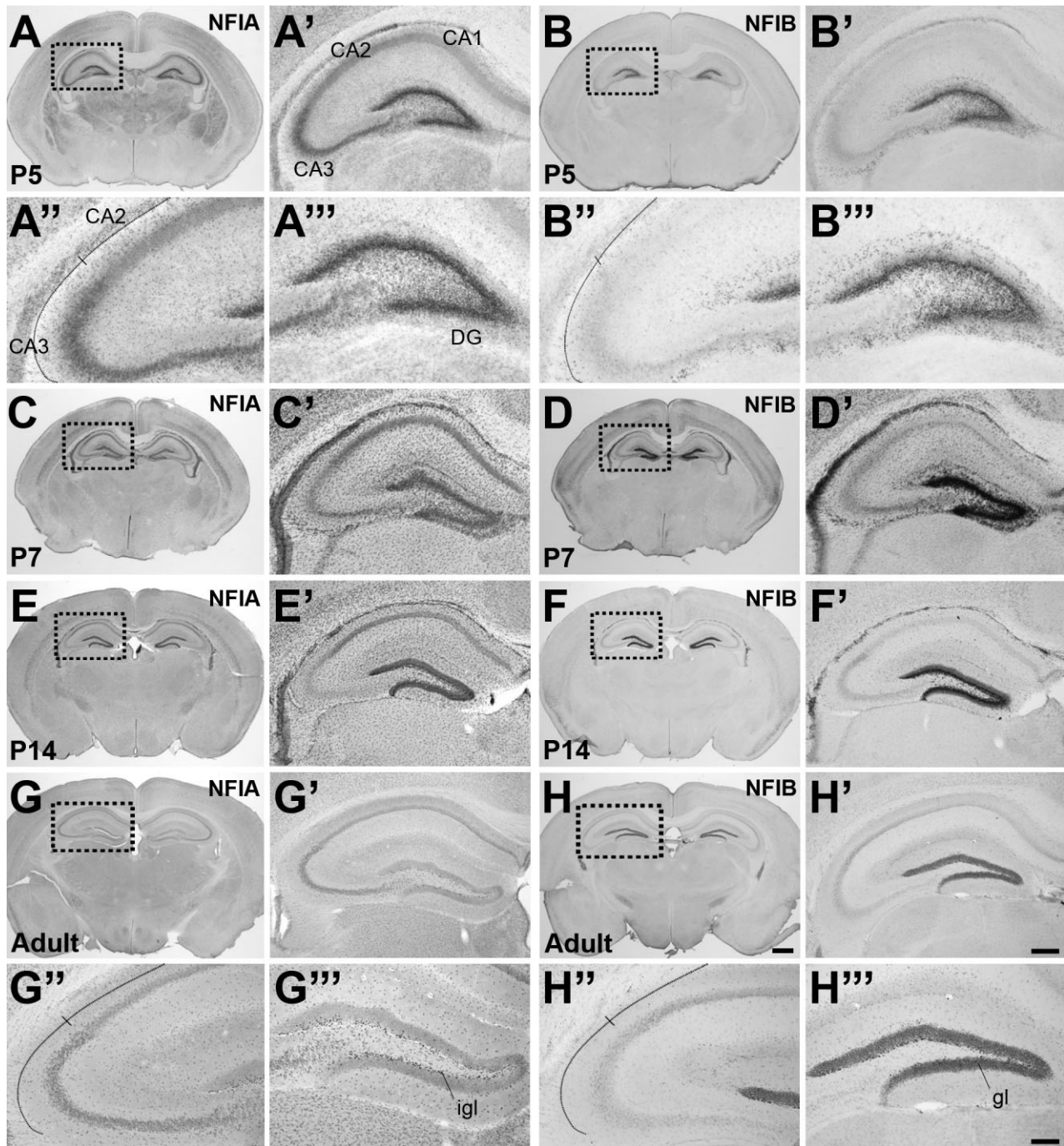


Fig. 11. Dynamic expression of NFI proteins in the postnatal and adult hippocampus. NFI proteins were strongly expressed in the hippocampus at postnatal stages. At P5 NFIA was expressed in CA3, CA2, and the dentate gyrus (A and higher magnification in A'), but was more highly expressed in CA3 compared to CA2 (A', high-power view showing the boundary between CA3 and CA2). At P5 the dentate gyrus highly expresses both NFIA (A'') and NFIB (B'') proteins. The strong expression of NFIB in the dentate gyrus granule layer remained throughout development and in the adult (D', F', H'''), but was not expressed at high levels in other regions of the developing hippocampus. At P7 and P14, NFIA expression remained within the

dentate gyrus, but also in the CA1 and CA2 regions of the hippocampus (C, C' and E, E'). In the adult, NFIA expression declined, with low levels of expression in CA3 and CA2 (see boundary in panel G'') and in the inner granular layer of the dentate gyrus (G'''). NFIB expression in the adult hippocampus was high in the dentate gyrus and particularly in the granule layer (H'''). All sections shown are in the coronal plane. DG, dentate gyrus; CA, Ammon's horn; igl, inner granular layer; gl, granule layer. Scale bars = 600  $\mu$ m in H for A, B; 625  $\mu$ m for C, D; 700  $\mu$ m for E-H; 200  $\mu$ m in H' for A'-D'; 260  $\mu$ m for E', F'; 290  $\mu$ m for G', H'; 100  $\mu$ m in H'' for A''-B''; 150  $\mu$ m for G''-H''.

autonomous formation of this commissure. To investigate this, we used retrograde tracing to label neurons projecting across the midline and through the corpus callosum, and then colabeled for either NFIA or NFIB. Using this technique we demonstrated that from P2–5 NFIA is expressed in a small subpopulation of callosally projecting neurons. Thus, it is possible that NFIA plays a minor cell-autonomous role in the formation of the corpus callosum. However, this finding rather emphasizes the importance of NFIA in the development of axon guidance substrates at the midline for the proper formation of the corpus callosum (Shu et al., 2003). NFIB was not observed in any neurons that project across the corpus callosum at P2 or P5, suggesting that the failure of this commissure to form in *Nfib* knockout mice is largely due to the lack of midline glial substrates. However, we cannot rule out the possibility that NFIA and NFIB at some timepoint earlier than P2 had been expressed in callosally projecting neurons. These findings suggest that neither NFIA nor NFIB are involved in cell-autonomous regulation of corpus callosum formation, but that nonautonomous roles are crucial for the development of this structure. In addition, the expression of NFIA and NFIB in laterally projecting neurons suggests that these proteins may be involved in the regulation of corticofugal axon targeting. Together, our findings imply that NFIA and NFIB play various crucial roles in cortical development.

### Regulation of midline guidance structures by *Nfi* genes

Accurate formation of the substrate over which commissural axons grow is a prerequisite for the formation of large fiber tracts, including the corpus callosum and the hippocampal commissure. At the midline, the substrate is comprised of midline glial populations that constitute an intermediate target for growing commissural axons. NFIA colocalizes with GFAP in the GW and the IGG (Shu et al., 2003). In addition, the loss of midline glial populations has been demonstrated in both *Nfia*<sup>-/-</sup> and *Nfib*<sup>-/-</sup> mice, and these animals also display agenesis of major forebrain commissures (das Neves et al., 1999; Shu et al., 2003; Steele-Perkins et al., 2005). Therefore, the failure of commissures to form may be due to deficits in midline glial structures.

### Expression of NFI proteins throughout hippocampal development

Postnatal expression of *Nfia* and *Nfib* mRNA in the hippocampus has previously been described (Behrens et al., 2000). In this study, *Nfia* and *Nfib* expression was analyzed in the P9 mouse brain, and mRNA for both genes were observed in the dentate gyrus and in the CA1 region. Here we show that NFIA and NFIB proteins are expressed in specific cell populations of the developing hippocampus. Both proteins are expressed in the hippocampal primordium during early embryonic development, and then become restricted to specific regions of the hippocampus. Both NFIA and NFIB are highly expressed in the dentate gyrus from its formation and into postnatal stages. Importantly, *Nfib* knockout mice display hippocampal defects, including malformation of the dentate gyrus (Steele-Perkins et al., 2005). A similar hippocampal phenotype has been observed in *Emx2* knockout mice (Tole et al., 2000; Zhao et al., 2006), and microarray analysis in neural precursors identified *Nfia* as a downstream target of *Emx2*

(Gangemi et al., 2006). Another mouse mutant with similar hippocampal abnormalities is the LRP6 (low-density lipoprotein receptor-related protein)-deficient mice. These mice have a generalized defect in the Wnt/b-catenin signaling pathway, resulting in an impaired production of dentate granule cells along with abnormalities in the radial glial scaffold (Zhou et al., 2004). How NFI proteins regulate hippocampal development, however, requires further investigation.

## CONCLUSIONS

This study presents the first detailed description of NFI protein expression in the developing telencephalon. The data provide the basis for further functional studies of these molecules and how they may regulate telencephalic development. The highly dynamic pre- and postnatal expression of NFIA and NFIB, as well as their organized spatiotemporal expression patterns, suggest that different NFI proteins may regulate sequential developmental events in a given system. Also, it has been demonstrated that these proteins may be further modulated posttranslationally (Bandyopadhyay and Gronostajski, 1994). Analyzing such modifications, as well as identifying upstream effectors and downstream targets of NFI proteins is crucial to determining the context-specific roles of these proteins during telencephalic development.

Both *Nfia* and *Nfib* knockout mice display agenesis of the corpus callosum and a malformed hippocampal commissure as well as severe defects in the formation of midline glial populations. Here, we have revealed a highly dynamic developmental expression of both proteins in cortex and hippocampus. Our findings, however, reveal that in the cortex, NFIA and NFIB are not predominantly expressed in neurons that project across the midline, but rather in laterally projecting neurons. These results indicate that the defects in commissural formation observed in the mutant mice are likely due to nonautonomous processes, such as regulation of axon guidance substrates within the cortex and at the telencephalic midline. As for the expression in neurons projecting laterally, the role of NFIA and NFIB remains to be determined.

## ACKNOWLEDGMENTS

The authors thank Sarah Baer from Active Motif from help in obtaining the Nfi antibodies. L.J.R. is an NHMRC Senior Research Fellow, M.P. holds an NHMRC Howard Florey Centenary Research Fellowship, and R.M. holds an NHMRC CJ Martin Fellowship.

## LITERATURE CITED

- Apt D, Liu Y, Bernard HU. 1994. Cloning and functional analysis of spliced isoforms of human nuclear factor I-X: interference with transcriptional activation by NFI/CTF in a cell-type specific manner. *Nucleic Acids Res* 22:3825–3833.
- Bandyopadhyay S, Gronostajski RM. 1994. Identification of a conserved oxidation-sensitive cysteine residue in the NFI family of DNA-binding proteins. *J Biol Chem* 269:29949–29955.
- Bayer SA. 1980. Development of the hippocampal region in the rat. I. Neurogenesis examined with 3H-thymidine autoradiography. *J Comp Neurol* 190:87–114.
- Behrens M, Venkatraman G, Gronostajski RM, Reed RR, Margolis FL. 2000. NFI in the development of the olfactory neuroepithelium and the

- regulation of olfactory marker protein gene expression. *Eur J Neurosci* 12:1372–1384.
- Bishop KM, Goudreau G, O'Leary DD. 2000. Regulation of area identity in the mammalian neocortex by *Emx2* and *Pax6*. *Science* 288:344–349.
- Britz O, Mattar P, Nguyen L, Langevin LM, Zimmer C, Alam S, Guillemot F, Schuurmans C. 2006. A role for proneural genes in the maturation of cortical progenitor cells. *Cereb Cortex* 16(Suppl 1):i138–151.
- Chaudhry AZ, Lyons GE, Gronostajski RM. 1997. Expression patterns of the four nuclear factor I genes during mouse embryogenesis indicate a potential role in development. *Dev Dyn* 208:313–325.
- Cheng X, Hsu CM, Currle DS, Hu JS, Barkovich AJ, Monuki ES. 2006. Central roles of the roof plate in telencephalic development and holoprosencephaly. *J Neurosci* 26:7640–7649.
- das Neves L, Duchala CS, Tolentino-Silva F, Haxhiu MA, Colmenares C, Macklin WB, Campbell CE, Butz KG, Gronostajski RM. 1999. Disruption of the murine nuclear factor I-A gene (*Nfia*) results in perinatal lethality, hydrocephalus, and agenesis of the corpus callosum. *Proc Natl Acad Sci U S A* 96:11946–11951.
- Di Giorgi-Gerevini V, Melchiorri D, Battaglia G, Ricci-Vitiani L, Ciceroni C, Busceti CL, Biagioni F, Iacovelli L, Canudas AM, Parati E, De Maria R, Nicoletti F. 2005. Endogenous activation of metabotropic glutamate receptors supports the proliferation and survival of neural progenitor cells. *Cell Death Differ* 12:1124–1133.
- Gangemi RM, Daga A, Muzio L, Marubbi D, Cocozza S, Perera M, Verardo S, Bordo D, Griffiro F, Capra MC, Mallamaci A, Corte G. 2006. Effects of *Emx2* inactivation on the gene expression profile of neural precursors. *Eur J Neurosci* 23:325–334.
- Gass P, Frankfurter A, Katsetos CD, Herman MM, Donoso LA, Rubinstein LJ. 1990. Antigenic expression of neuron-associated class III beta-tubulin isotype (h beta 4) and microtubule-associated protein 2 (MAP2) by the human retinoblastoma cell line WERI-Rb1. A comparative immunoblot and immunocytochemical study. *Ophthalmic Res* 22:57–66.
- Gil G, Smith JR, Goldstein JL, Slaughter CA, Orth K, Brown MS, Osborne TF. 1988. Multiple genes encode nuclear factor I-like proteins that bind to the promoter for 3-hydroxy-3-methylglutaryl-coenzyme A reductase. *Proc Natl Acad Sci U S A* 85:8963–8967.
- Gronostajski RM. 2000. Roles of the NFI/CTF gene family in transcription and development. *Gene* 249:31–45.
- Hand R, Bortone D, Mattar P, Nguyen L, Heng JI, Guerrier S, Boutt E, Peters E, Barnes AP, Parras C, Schuurmans C, Guillemot F, Polleux F. 2005. Phosphorylation of Neurogenin2 specifies the migration properties and the dendritic morphology of pyramidal neurons in the neocortex. *Neuron* 48:45–62.
- Hay RT. 1985. Origin of adenovirus DNA replication. Role of the nuclear factor I binding site in vivo. *J Mol Biol* 186:129–136.
- Holm PC, Mader MT, Haubst N, Wizenmann A, Sigvardsson M, Gotz M. 2007. Loss- and gain-of-function analyses reveal targets of *Pax6* in the developing mouse telencephalon. *Mol Cell Neurosci* 34:99–119.
- Hurwitz J, Adhya S, Field J, Gronostajski R, Guggenheimer RA, Kenny M, Lindenbaum J, Nagata K. 1985. Synthesis of adenoviral DNA with purified proteins. Marks PA, editor. New York: Academic Press. p 15–24.
- Inoue T, Tamura T, Furuichi T, Mikoshiba K. 1990. Isolation of complementary DNAs encoding a cerebellum-enriched nuclear factor I family that activates transcription from the mouse myelin basic protein promoter. *J Biol Chem* 265:19065–19070.
- Kruse U, Sippel AE. 1994. Transcription factor nuclear factor I proteins form stable homo- and heterodimers. *FEBS Lett* 348:46–50.
- Leegwater PA, van Driel W, van der Vliet PC. 1985. Recognition site of nuclear factor I, a sequence-specific DNA-binding protein from HeLa cells that stimulates adenovirus DNA replication. *EMBO J* 4:1515–1521.
- Luskin MB, Shatz CJ. 1985. Studies of the earliest generated cells of the cat's visual cortex: cogeneration of subplate and marginal zones. *J Neurosci* 5:1062–1075.
- Mallamaci A, Iannone R, Briata P, Pintonello L, Mercurio S, Boncinelli E, Corte G. 1998. *EMX2* protein in the developing mouse brain and olfactory area. *Mech Dev* 77:165–172.
- Mallamaci A, Muzio L, Chan CH, Parnavelas J, Boncinelli E. 2000. Area identity shifts in the early cerebral cortex of *Emx2*<sup>-/-</sup> mutant mice. *Nat Neurosci* 3:679–686.
- Marin-Padilla M. 1998. Cajal-Retzius cells and the development of the neocortex. *Trends Neurosci* 21:64–71.
- Mattar P, Britz O, Johannes C, Nieto M, Ma L, Rebeyka A, Klenin N, Polleux F, Guillemot F, Schuurmans C. 2004. A screen for downstream effectors of Neurogenin2 in the embryonic neocortex. *Dev Biol* 273:373–389.
- Meisterernst M, Rogge L, Donath C, Gander I, Lottspeich F, Mertz R, Dobner T, Fockler R, Stelzer G, Winnacker EL. 1988. Isolation and characterization of the porcine nuclear factor I (NFI) gene. *FEBS Lett* 236:27–32.
- Monuki ES, Porter FD, Walsh CA. 2001. Patterning of the dorsal telencephalon and cerebral cortex by a roof plate-Lhx2 pathway. *Neuron* 32:591–604.
- Mullen RJ, Buck CR, Smith AM. 1992. NeuN, a neuronal specific nuclear protein in vertebrates. *Development (Cambridge, UK)* 116:201–211.
- Muzio L, Mallamaci A. 2003. *Emx1*, *emx2* and *pax6* in specification, regionalization and arealization of the cerebral cortex. *Cereb Cortex* 13:641–647.
- Muzio L, DiBenedetto B, Stoykova A, Boncinelli E, Gruss P, Mallamaci A. 2002a. Conversion of cerebral cortex into basal ganglia in *Emx2*<sup>(-/-)</sup> *Pax6*(Sey/Sey) double-mutant mice. *Nat Neurosci* 5:737–745.
- Muzio L, DiBenedetto B, Stoykova A, Boncinelli E, Gruss P, Mallamaci A. 2002b. *Emx2* and *Pax6* control regionalization of the pre-neuronogenic cortical primordium. *Cereb Cortex* 12:129–139.
- Nagata K, Guggenheimer RA, Enomoto T, Lichy JH, Hurwitz J. 1982. Adenovirus DNA replication in vitro: identification of a host factor that stimulates synthesis of the preterminal protein-dCMP complex. *Proc Natl Acad Sci U S A* 79:6438–6442.
- Paonessa G, Gounari F, Frank R, Cortese R. 1988. Purification of a NF1-like DNA-binding protein from rat liver and cloning of the corresponding cDNA. *EMBO J* 7:3115–3123.
- Rosenfeld PJ, O'Neill EA, Wides RJ, Kelly TJ. 1987. Sequence-specific interactions between cellular DNA-binding proteins and the adenovirus origin of DNA replication. *Mol Cell Biol* 7:875–886.
- Rupp RA, Kruse U, Multhaup G, Gobel U, Beyreuther K, Sippel AE. 1990. Chicken NFI/TGGCA proteins are encoded by at least three independent genes: NFI-A, NFI-B and NFI-C with homologues in mammalian genomes. *Nucleic Acids Res* 18:2607–2616.
- Santoro C, Mermod N, Andrews PC, Tjian R. 1988. A family of human CCAAT-box-binding proteins active in transcription and DNA replication: cloning and expression of multiple cDNAs. *Nature* 334:218–224.
- Seth A, Culverwell J, Walkowicz M, Toro S, Rick JM, Neuhauss SC, Varga ZM, Karlstrom RO. 2006. *Belladonna*(*Ihx2*) is required for neural patterning and midline axon guidance in the zebrafish forebrain. *Development (Cambridge, UK)* 133:725–735.
- Shu T, Richards LJ. 2001. Cortical axon guidance by the glial wedge during the development of the corpus callosum. *J Neurosci* 21:2749–2758.
- Shu T, Butz KG, Plachez C, Gronostajski RM, Richards LJ. 2003. Abnormal development of forebrain midline glia and commissural projections in *Nfia* knock-out mice. *J Neurosci* 23:203–212.
- Silver J, Lorenz SE, Wahlsten D, Coughlin J. 1982. Axonal guidance during development of the great cerebral commissures: descriptive and experimental studies, in vivo, on the role of preformed glial pathways. *J Comp Neurol* 210:10–29.
- Silver J, Edwards MA, Levitt P. 1993. Immunocytochemical demonstration of early appearing astroglial structures that form boundaries and pathways along axon tracts in the fetal brain. *J Comp Neurol* 328:415–436.
- Steele-Perkins G, Plachez C, Butz KG, Yang G, Bachurski CJ, Kinsman SL, Litwack ED, Richards LJ, Gronostajski RM. 2005. The transcription factor gene *Nfib* is essential for both lung maturation and brain development. *Mol Cell Biol* 25:685–698.
- Stoykova A, Gruss P. 1994. Roles of *Pax*-genes in developing and adult brain as suggested by expression patterns. *J Neurosci* 14(3 Pt 2):1395–1412.
- Tole S, Goudreau G, Assimacopoulos S, Grove EA. 2000. *Emx2* is required for growth of the hippocampus but not for hippocampal field specification. *J Neurosci* 20:2618–2625.
- Wang K, Pearson GD. 1985. Adenovirus sequences required for replication in vivo. *Nucleic Acids Res* 13:5173–5187.
- Wolf HK, Buslei R, Schmidt-Kastner R, Schmidt-Kastner PK, Pietsch T, Wiestler OD, Blumcke I. 1996. NeuN: a useful neuronal marker for diagnostic histopathology. *J Histochem Cytochem* 44:1167–1171.
- Xie Y, Skinner E, Landry C, Handley V, Schonmann V, Jacobs E, Fisher R, Campagnoni A. 2002. Influence of the embryonic preplate on the organization of the cerebral cortex: a targeted ablation model. *J Neurosci* 22:8981–8991.
- Zhao T, Kraemer N, Oldekamp J, Cankaya M, Szabo N, Conrad S, Skutella T, Alvarez-Bolado G. 2006. *Emx2* in the developing hippocampal fissure region. *Eur J Neurosci* 23:2895–2907.
- Zhou CJ, Zhao C, Pleasure SJ. 2004. Wnt signaling mutants have decreased dentate granule cell production and radial glial scaffolding abnormalities. *J Neurosci* 24:121–126.